Rapid Communications | Editors' Suggestion

Experimental search for the origin of low-energy modes in topological materials

G. P. Mazur,[1,*] K. Dybko,[1,2,†] A. Szczerbakow,[2] J. Z. Domagala,[2] A. Kazakov,[1] M. Zgirski,[2] E. Lusakowska,[2] S. Kret,[2] J. Korczak,[1,2] T. Story,[2] M. Sawicki,[2] and T. Dietl[1,3,‡]

[1]*International Research Centre MagTop, Institute of Physics, Polish Academy of Sciences, Aleja Lotnikow 32/46, PL-02668 Warsaw, Poland*

[2]*Institute of Physics, Polish Academy of Sciences, PL-02668 Warsaw, Poland*

[3]*WPI-Advanced Institute for Materials Research, Tohoku University, Sendai 980-8577, Japan*

(Received 14 December 2018; revised manuscript received 22 March 2019; published 26 July 2019)

Point-contact spectroscopy of several nonsuperconducting topological materials reveals a low-temperature phase transition that is characterized by a Bardeen-Cooper-Schrieffer type of criticality. We find such a behavior of differential conductance for topological surfaces of nonmagnetic and magnetic $Pb_{1-y-x}Sn_yMn_xTe$. We examine a possible contribution from superconducting nanoparticles, and show to what extent our data are consistent with Brzezicki's *et al.* theory (arXiv:1812.02168), assigning the observations to a collective state adjacent to atomic steps at topological surfaces.

DOI: 10.1103/PhysRevB.100.041408

Introduction. A series of point-contact experiments has revealed the existence of low-energy modes at the junctions of metal tips with topological semiconductors and semimetals [1–9]. Surprisingly, despite the absence of global superconductivity in these systems, the features in dI/dV decay critically with temperature and the magnetic field, in accord with the Bardeen-Cooper-Schrieffer (BCS) theory. It has therefore been concluded that the superconductivity results from tip-induced strain. In the case of Cd_3As_2 this interpretation appears to be supported by the featureless spectrum in the case of a soft point contact produced by silver paint [3,6]. Surprisingly, however, Andreev reflection-type spectra were recently reported for Au/Cd_3As_2 junctions (with neither a four-probe zero-resistance state nor the Meissner effect) [8], as well as for topological semimetals $MoTe_2$ [7] and WC [9] with hard and soft point contacts [7] of various nonmagnetic and magnetic metals [9]. A timely question then arises about the properties of other materials, such as topological crystalline insulators (TCIs) [10–14] in which hard point-contact characteristics reveal zero-bias conductance peaks (ZBCPs) [1].

Here, we show, employing a soft point-contact method, that a conductance gap with a broad ZBCP or Andreev-type characteristics develops at junctions of Ag with topological surfaces of diamagnetic, paramagnetic, and ferromagnetic $Pb_{1-y-x}Sn_yMn_xTe$, where $y \gtrsim 0.67$ and $0 \leqslant x \leqslant 0.10$, in which no signs of superconductivity are found. Nevertheless, the temperature dependence of the gap shows a BCS-like critical behavior as a function of temperature T and the magnetic field H with T_c up to 4.5 K and $\mu_0 H_c$ up to 3 T, independent of the orientation of the magnetic field with respect to the surface plane. This implies the emergence of a collective low-temperature phase whose appearance is insensitive not only to the magnetic state of the metallic part of the junction, as found previously [1,9], but also to the magnetic character of the topological material. In order to elucidate the nature of these striking observations, we put forward two models.

First, previous studies of the materials in question revealed superconductivity associated with metal nanoprecipitates [15] or misfit dislocations at the heterostructure interfaces [16,17]. Furthermore, studies of Pb/(Pb,Sn)Te junctions point to the presence of Sn diffusion in Pb [18], which raises the question on whether such an effect could generate superconducting Pb or Sn at the interface. It might be also anticipated that strain associated with different thermal expansion coefficients of silver paint and the samples or hard tips could generate misfit dislocations or precipitates. However, a series of auxiliary high-sensitivity magnetization and resistance measurements as well as high-resolution structural investigations of our samples have not revealed the presence of superconducting nanoparticles within our experimental resolution.

Second, a possible origin of a local collective phase at topological surfaces has recently been proposed by Brzezicki, Wysokiński, and Hyart (BWH) [19], who noted that the electronic structure of one-dimensional (1D) states at atomic steps in TCIs, revealed by scanning tunneling microscopy [20,21], is significantly richer than anticipated previously [20–23]. According to BWH, these 1D states may show by a low-temperature Peierls-like instability, leading to the appearance of low-energy excitations associated with topological states at the domains walls of the collective phase. We discuss to what extent our data are consistent with the BWH model and a possible microscopic nature of the collective phase.

Samples. We investigate here single crystals of rocksalt $Pb_{1-y}Sn_yTe$ and $Pb_{1-y-x}Sn_yMn_xTe$ obtained via the self-selecting vapor growth method [12,24] and the Bridgman technique [25], respectively. Results of electric, magnetic, x-ray, and electron transmission microscopy characterizations of the studied samples are presented in the Supplemental Material [26]. We study samples with $y = 0$, 0.2, 0.67, 0.74, 0.8, and 1, which covers both the topologically trivial and nontrivial ranges, as the TCI phase occurs for $y \gtrsim 0.30$ [14].

*grzegorz.mazur@MagTop.ifpan.edu.pl
†dybko@ifpan.edu.pl
‡dietl@MagTop.ifpan.edu.pl

According to both angle-resolved photoemission [13,14,27] and magnetotransport investigations [28], the surface topological cones coexist with bulk states even for high bulk carrier densities specific to these systems. At the same time, the energetic position of the surface-cone neutrality points with respect to the Fermi level depends on the character of the surface states and the degree of surface oxidation, the questions under investigation now [29,30]. The search for metal precipitates by x-ray diffraction and electron microscopy, also in the vicinity of dislocations, has not revealed the presence of any nanoclustering within the state-of-the-art resolution [26].

According to the results of magnetization measurements [26], carried out by employing a superconducting quantum interference device (SQUID), nonmagnetic compounds show a field-independent diamagnetic susceptibility, enhanced by strong interband polarization in the inverted band structure case. The Mn-doped samples contain a Sn concentration corresponding to the TCI phase and a bulk hole density high enough to populate 12 Σ valleys. A large density of states (DOS) associated with these valleys makes hole-mediated exchange coupling between Mn ions sufficiently strong to drive the ferromagnetic ordering [25,31]. The Curie temperature T_{Curie}, separating the paramagnetic and ferromagnetic phase, is 2.7 and 14 K for Mn concentrations $x = 0.03$ and 0.10, and Sn contents $y = 0.67$ and 0.74, respectively [26]. These values are consistent with the mean-field *p-d* Zener model [26,32,33].

Point-contact spectroscopy. We employ the soft point-contact method [34–36], in which a 15-μm Au wire is fixed by silver paint. As shown in Fig. 1(a), $dI/dV(V)$ is featureless in the case of the topologically trivial materials PbTe and $Pb_{0.80}Sn_{0.20}Te$. However, in the case of the diamagnetic TCI $Pb_{0.20}Sn_{0.80}Te$ we find at low temperatures $T < T_c$ and magnetic fields $H < H_c$ maxima (ZBCP) centered at $V = 0$ and superimposed on a conductance gap (see also the data in Ref. [26]). As observed in other systems [1–6,8,9], the spectra forms vary from contact to contact [26]. In the thermal regime they change over time in a jump way as well as can be modified by current pulses across the point contact [26,34].

Within the point-contact theories [34], the enhanced junction conductance at $T < T_c$ and at $V \approx 0$, i.e., the presence of ZBCP, can be interpreted in terms of the Andreev reflection (pointing to superconductivity) or to an enlarged DOS due to the appearance of, for instance, zero modes at $T < T_c$ [19]. In either of these scenarios current heating at higher bias voltages may result in side minima [37]. Within the superconductivity models, such a spectrum is typical for the thermal regime, i.e., when the contact diameter is larger than the inelastic diffusion length [34] [Fig. 1(c)]. In the opposite limit, spectroscopic information is not blurred, and side maxima in dI/dV, reflecting the DOS enlargement at the gap edges, provide the value of the relevant gap. Within such an approach the data in Fig. 1(b) (see also Ref. [26]) correspond to the spectroscopic regime. An interesting question arises on whether such a phenomenology can be directly applied to other gapped collective states, such as the one proposed by BWH [19].

According to Fig. 2, dI/dV shows clear spectroscopic features in magnetic crystals. The spectrum for

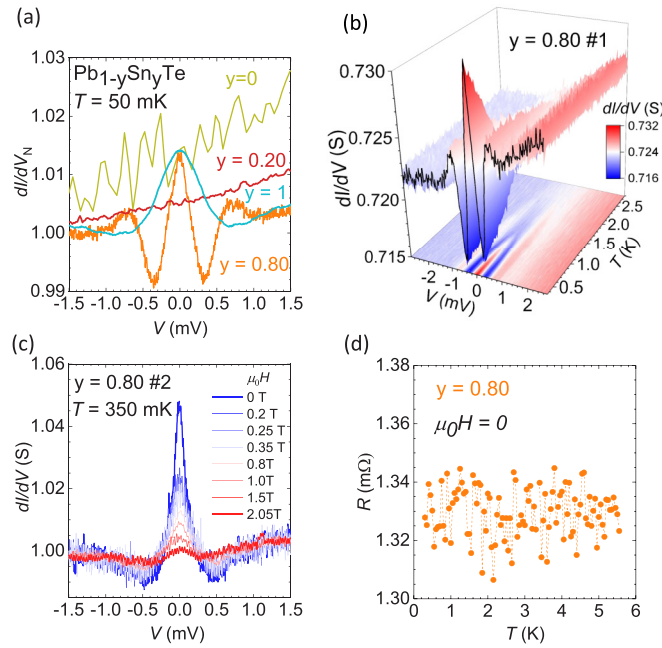

FIG. 1. (a) Differential conductance dI/dV at 50 mK normalized to its value at the normal state for the as-grown (001) $Pb_{1-y}Sn_yTe$ with $y = 0$, 0.20, 0.80, and 1. The spectrum is featureless for $y = 0$ (PbTe) and $y = 0.20$ but shows zero-energy mode characteristics for Sn content ($y = 0.80$ and 1, i.e., SnTe) corresponding to a topological crystalline insulator phase. Evolution of the spectrum with temperature (b) and the magnetic field (c) for $y = 0.80$ and two locations of the point contact on the sample surface, respectively. A magnetic field is applied perpendicularly to the (001) plane. (d) Resistance of this sample measured by a four-contact method with a current density as low as 2.5×10^{-3} A/cm^2. No global superconductivity is detected.

$Pb_{0.3}Sn_{0.67}Mn_{0.03}Te$ [Fig. 2(a)] exhibits a gap with a small zero-bias peak vanishing smoothly with increasing temperature. For a cleaved (100) surface of $Pb_{0.16}Sn_{0.74}Mn_{0.10}Te$, a splitting of ZBCP, resembling Andreev reflection characteristics in the spectroscopic regime and for a nonzero barrier transparency [34], has been detected [Fig. 2(c)].

Importantly, temperature and magnetic field ranges in which these spectroscopic features appear are rather enhanced compared to nonmagnetic crystals. This is best seen in Fig. 3 that depicts the contact resistance and a half of the energy distance between conductance maxima $\Delta(T, H)$ for all studied samples with a high Sn content. Furthermore, according to Fig. 3, $\Delta(T)$ is quite well described by an interpolation formula of the BCS expression, $\Delta(T) = Ck_BT_c[1 - (T/T_c)^{3.3}]^{0.5}$, where C in our case is more than twofold greater than the BCS value $C = 1.76$. Similarly, a reasonable account of $\Delta(H)$ data is obtained by using another interpolation formula suitable for type-II superconductors, $\Delta(T, H) = \Delta(T, H = 0)(1 - H/H_c)^{1/2}$. This description of $\Delta(T, H)$ holds for the diamagnetic $Pb_{0.2}Sn_{0.80}Te$, ferromagnetic $Pb_{0.16}Sn_{0.74}Mn_{0.10}Te$, and across the paramagnetic-ferromagnetic phase boundary, the case of $Pb_{0.20}Sn_{0.67}Mn_{0.03}Te$, in which $T_c > T_{\mathrm{Curie}}$. The existence of a transition to another phase is also documented

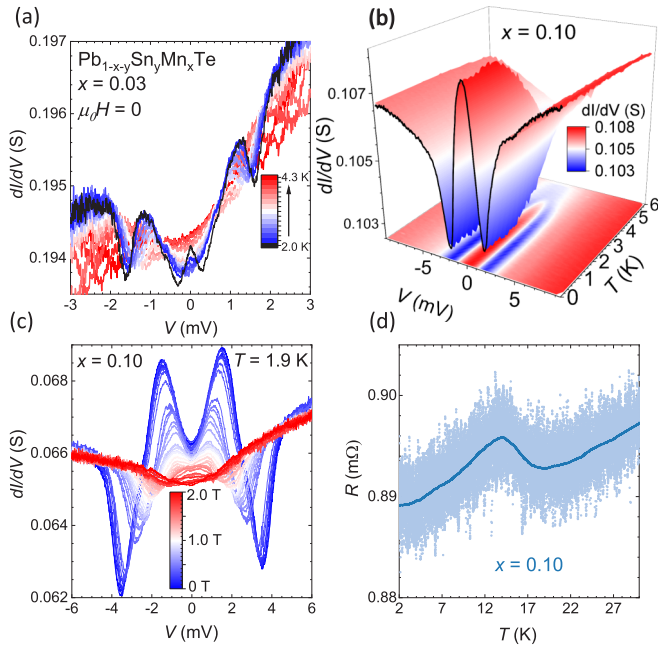

FIG. 2. Temperature dependence of differential conductance spectra for the etched (011) $Pb_{0.30}Sn_{0.67}Mn_{0.03}Te$ (a) in a spectroscopic regime and (011) $Pb_{0.16}Sn_{0.74}Mn_{0.10}Te$ (b) in a thermal regime, respectively. (c) Evolution of the spectrum with the magnetic field at 1.8 K for the cleaved (001) $Pb_{0.16}Sn_{0.74}Mn_{0.10}Te$ in a spectroscopic regime. A magnetic field is applied perpendicularly to the sample plane. (d) Resistance of $Pb_{0.16}Sn_{0.74}Mn_{0.10}Te$ measured by a four-contact method with current density 2.5×10^{-5} A/cm^2 (noisy trace), and the solid line represents a numerical average over 40 temperature scans. Critical scattering at the Curie temperature $T_{\text{Curie}} = 14$ K is observed but no global superconductivity is detected.

by a kink in the temperature dependence of the differential resistance for $V \to 0$ at T_c, as shown in Fig. 3(a).

The accumulated results demonstrate, therefore, the appearance in junctions of the normal metal with diamagnetic, paramagnetic, and ferromagnetic IV-VI TCIs of another phase below T_c and H_c, which is characterized by an energy gap and excitations residing near its center. The presence of a phase transition rules out the Kondo effect [38–41] and the Coulomb gap [42,43] as the mechanisms accounting for the observed features. Similarly, the absence of global superconductivity without metal layers [Figs. 1(d) and 2(d) as well as data in Ref. [26]] indicates that unconventional two-dimensional (2D) superconductivity associated with surface topological states [44] or dislocation arrays [45] in TCIs does not appear under our experimental conditions. The absence of 2D superconductivity is also documented by similar values of H_c for the magnetic field perpendicular and parallel to the surface [26].

Role of superconducting precipitates. According to comprehensive structural and SQUID studies, magnetic nanoparticles account for high T_{Curie} ferromagnetism observed in a number of semiconductors and oxides over the last two decades [46]. Similarly to the ferromagnetic case, embedded nanoparticles can show a variety of superconducting characteristics, such as the Meissner effect, which may depend on nanoparticle chemical composition, strain, and size [15–17,47,48]. Here, the presence of superconducting precipitates that could give rise to local superconductivity is ruled out, within an experimental accuracy of 0.1 ppm, by high-sensitivity beyond state-of-the-art SQUID magnetometry [26,49]. Furthermore, no precipitates have been revealed by state-of-the-art x-ray diffraction and transmission microscopy measurements [26]. Similarly, no indications of superconductivity have been found in topological samples covered entirely by the silver paint or containing a deposited silver film [26], pointing to the absence of both interfacial superconductivity and superconducting inclusions at the metal/semiconductor interface.

Role of surface atomic steps. Figure 4 presents the surface morphology of our single crystals under ambient conditions, determined by atomic force microscopy (AFM). As seen in Figs. 4(a) and 4(b), (001) facets of as-grown $Pb_{0.20}Sn_{0.80}Te$ contain atomically flat 0.5-μm-wide terraces, terminated by monoatomic steps. Similarly, Figs. 4(c) and 4(d) visualize a (001) surface of cleaved $Pb_{0.16}Sn_{0.74}Mn_{0.10}Te$ showing a larger roughness and multilayer steps. Results in Figs. 1(b)

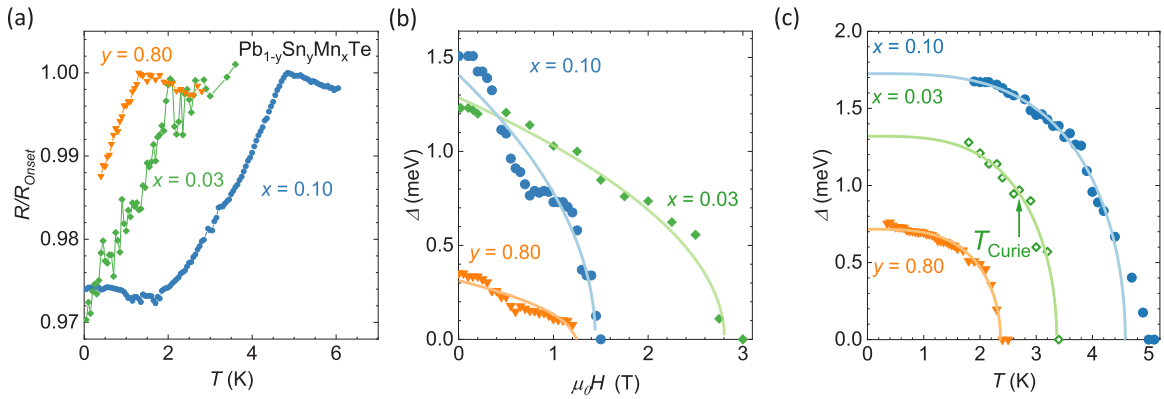

FIG. 3. (a) Temperature dependence of the point-contact resistance at the limit of zero bias pointing to a phase transition. (b), (c) Conductance gap Δ evaluated from the differential conductance spectra for samples presented in Figs. 1 and 2 for $Pb_{1-y-x}Sn_yMn_xTe$ corresponding to the topological crystalline insulator phase vs magnetic field perpendicular to the surface plane and temperature, respectively. Solid lines in (b) are fits to $\Delta(T, H) = \Delta(T, H = 0)(1 - H/H_c)^{1/2}$. Solid lines in (c) are fits of the BCS formula for $\Delta(T)$ to the experimental points treating T_c and C as adjustable parameters ($C = 4.35$, 4.53, and 3.49 from top to bottom, respectively; $C = 1.76$ in the BCS theory).

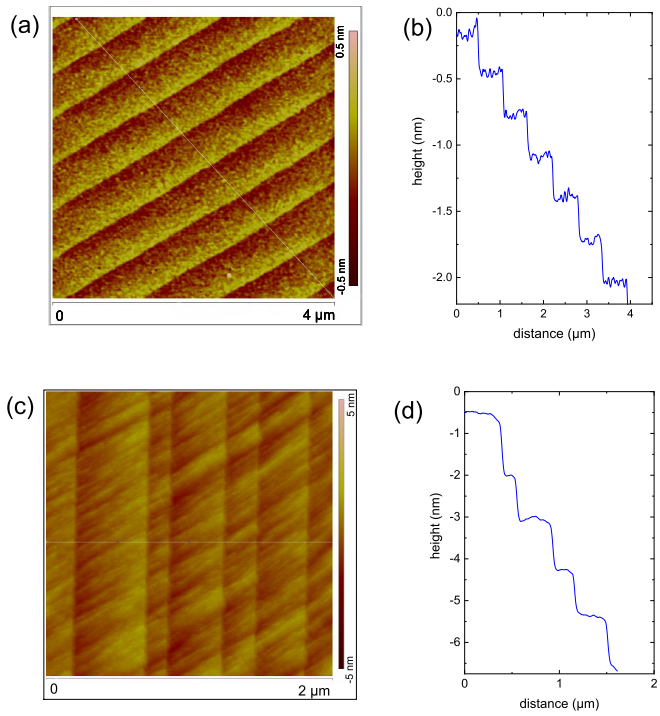

FIG. 4. AFM images of the studied single-crystal surfaces. (a) Naturally grown (001) facet of $Pb_{0.20}Sn_{0.80}Te$ showing surface steps. (c) Cleaved (001) surface of $Pb_{0.16}Sn_{0.74}Mn_{0.10}Te$ showing multilayer steps and a higher roughness. (b) and (d) depict step height profiles. The obtained values of about 0.3 nm in (b) correspond to a single atomic step (315 pm).

and 1(c), and 2(c) were actually taken for these two surfaces, respectively. We claim that a collective low-temperature phase of the carrier liquid occupying 1D topological step states [19–23] may account for the differential conductance spectra reported here. According to AFM micrographs, a single Ag grain extends over a dozen steps. The magnitude of ZBCP, about 50–500e^2/h, is consistent with the fact that several grains participate in the charge transport process.

The above interpretation requires the Fermi level of our *p*-type samples to reside within the 1D states, whereas tight-binding computations place the 1D band in the gap [19–23]. We note, however, that our experimental method implies the formation of Schottky's metal-semiconductor junction, which leads usually to the Fermi level pinning in the band gap region at the semiconductor surface [50]. This effect, together with a considerable width of the 1D band, as predicted by the BWH theory [19], make the partial occupation of the 1D states plausible. The depletion in the bulk carrier density implies also that Mn spins adjacent to the surface will be rather coupled by antiferromagnetic superexchange [51] than by the hole-mediated ferromagnetic interactions dominating in the bulk [25,26].

However, since the Fermi liquid is unstable in the 1D case, one expects the emergence of a collective state at low temperatures driven by carrier correlation, presumably enhanced by coupling to phonons and localized spins. For a class of electronic instabilities, such as superconductivity and charge/spin density waves, the BCS relation between the gap 2Δ and the critical temperature T_c remains valid within the mean-field approximation. However, because of the dominating role played by thermal and quantum fluctuations of the order parameter, the apparent magnitude of T_c becomes much reduced in the 1D case [52,53]. This explains the enhanced magnitude of C over the BCS value (Fig. 3) but indicates also that 1D surface states may not support superconductivity with T_c as high as 5 K.

As demonstrated by BWH [19], the 1D states adjacent to the surface atomic step show a much more abundant spectrum than anticipated previously [20–23]. Within this insight, the effects of magnetic instabilities have been considered and the nature of low-energy excitations proposed [19]. In analogy with the Su-Schreffer-Heeger model [54], the low-energy modes are associated with domain walls between the regions characterized by the opposite directions of the order parameter for which, as proven, topological invariants differ. These walls, and thus low-energy excitations, vanish in the magnetic field with a rate determined by a competition of the carrier-carrier exchange coupling with the Zeeman, spin-orbit, and *sp-d* exchange interactions. Depending on the assumed broadening, the evaluated conductance spectra show a single ZBCP, or a more complex peak structure that reflects the multimode excitation spectrum and may resemble Andreev reflection [19].

Summary and outlook. Our results on soft point-contact spectroscopy bring to light the existence of a low-temperature phase in lead-tin and lead-tin-manganese tellurides with the tin content corresponding to the topological phase, which substantiates the universality of the phenomenon [1–6,8,9]. The findings could be explained by the presence of superconducting nanoparticles, the surface topological states playing only an ancillary role. However, no indications for the formation of nanoparticles have so far been found. At the same time, our experiments do not provide evidence for the presence of superconductivity at the interface between the metal and the TCI. Hence, this phase can be also linked to carriers occupying 1D topological states adjacent to surface atomic steps, which undergo a transition to a collective state at sufficiently low temperatures and magnetic fields. Four microprobe measurements of conductance along individual steps in materials with the Fermi level within the step states are expected to demonstrate whether this collective phase is a 1D superconductor or a 1D gapped insulator with low-energy excitations at the domain walls. Future work will show to what extent the unusual properties associated with the presence of 1D and 0D topological states offer interesting functionalities.

Acknowledgments. We thank M. Foltyn and P. Skupinski for technical support and V. Galitski for a valuable discussion. The Research Foundation MagTop–International Centre for Interfacing Magnetism and Superconductivity with Topological Matter (short name: International Research Centre MagTop) is funded by the Foundation for Polish Science through the IRA Programme financed by the EU within SG OP Programme. The work at the Institute of Physics, Polish Academy of Sciences was supported by the National Science Center (Poland) through the following Grants: PRELUDIUM (2015/19/N/ST3/02626), OPUS (2012/07/B/ST3/03607, 2013/09/B/ST3/04175,

2014/15/B/ST3/03833, 2017/27/B/ST3/02470), and MAESTRO (2011/02/A/ST3/00125). The transmission electron microscopy/focused ion beam (TEM/FIB) investigation was performed on equipment supported by the Polish Government under Agreement No. 4277/E-67/SPUB/2017/1.

[1] S. Das, L. Aggarwal, S. Roychowdhury, M. Aslam, S. Gayen, K. A. Biswas, and G. Sheet, Unexpected superconductivity at nanoscale junctions made on the topological crystalline insulator $Pb_{0.6}Sn_{0.4}Te$, Appl. Phys. Lett. **109**, 132601 (2016).

[2] L. Aggarwal, A. Gaurav, G. S. Thakur, Z. Haque, A. K. Ganguli, and G. Sheet, Unconventional superconductivity at mesoscopic point contacts on the 3D Dirac semimetal Cd_3As_2, Nat. Mater. **15**, 32 (2016).

[3] H. Wang, H. Wang, H. Liu, H. Lu, W. Yang, S. Jia, X.-J. Liu, X. C. Xie, J. Wei, and J. Wang, Observation of superconductivity induced by a point contact on 3D Dirac semimetal Cd_3As_2 crystals, Nat. Mater. **15**, 38 (2016).

[4] L. Aggarwal, S. Gayen, S. Das, R. Kumar, S. Vicky, C. Felser, C. Shekgar, and G. Sheet, Mesoscopic superconductivity and high spin polarization coexisting at metallic point contacts on Weyl semimetal TaAs, Nat. Commun. **8**, 13974 (2017).

[5] H. Wang, H. Wang, Y. Chen, J. Luo, Z. Yuan, J. Liu, Y. Wang, S. Jia, X.-J. Liu, J. Wei, and J. Wang, Discovery of tip induced unconventional superconductivity on Weyl semimetal, Sci. Bull. **62**, 425 (2017).

[6] H. Wang, L. Ma, and J. Wang, Tip-induced or enhanced superconductivity: A way to detect topological superconductivity, Sci. Bull. **63**, 1141 (2018).

[7] Y. Naidyuk, O. Kvitnitskaya, D. Bashlakov, S. Aswartham, I. Morozov, I. Chernyavskii, G. Fuchs, S.-L. Drechsler, R. Hühne, K. Nielsch, B. Büchner, and D. Efremov, Surface superconductivity in the Weyl semimetal $MoTe_2$ detected by point contact spectroscopy, 2D Mater. **5**, 045014 (2018).

[8] O. O. Shvetsov, V. D. Esin, A. V. Timonina, N. N. Kolesnikov, and E. V. Deviatov, Surface superconductivity in a three-dimensional Cd_3As_2 semimetal at the interface with a gold contact, Phys. Rev. B **99**, 125305 (2019).

[9] W. L. Zhu, X. Y. Hou, J. Li, Y. F. Huang, S. Zhang, J.B. He, D. Chen, M. D. Zhang, H. X. Yang, Z. A. Ren, J. P. Hu, L. Shan, and G. F. Chen, Evidence of interfacial topological superconductivity on the topological semimetal tungsten carbide induced by metal deposition, arXiv:1811.12129.

[10] L. Fu, Topological Crystalline Insulators, Phys. Rev. Lett. **106**, 106802 (2011).

[11] T. H. Hsieh, H. Lin, J. Liu, W. Duan, A. Bansil, and L. Fu, Topological crystalline insulators in the SnTe material class, Nat. Commun. **3**, 982 (2012).

[12] P. Dziawa, B. J. Kowalski, K. Dybko, R. Buczko, A. Szczerbakow, M. Szot, E. Łusakowska, T. Balasubramanian, B. M. Wojek, M. H. Berntsen, O. Tjernberg, and T. Story, Topological crystalline insulator states in $Pb_{1-x}Sn_xSe$, Nat. Mater. **11**, 1023 (2012).

[13] Y. Tanaka, Z. Ren, T. Sato, K. Nakayama, S. Souma, T. Takahashi, K. Segawa, and Y. Ando, Experimental realization of a topological crystalline insulator in SnTe, Nat. Phys. **8**, 800 (2012).

[14] S.-Y. Xu, C. Liu, N. Alidoust, M. Neupane, D. Qian, I. Belopolski, J. D. Denlinger, Y. J. Wang, L. A. W. H. Lin, G. Landolt, B. Slomski, J. H. Dil, A. Marcinkova, E. Morosan, Q. Gibson, R. Sankar, F. C. Chou, R. J. Cava, A. Bansil, and M. Z. Hasan, Observation of a topological crystalline insulator phase and topological phase transition in $Pb_{1-x}Sn_xTe$, Nat. Commun. **3**, 1192 (2012).

[15] S. D. Darchuk, L. A. Korovina, F. F. Sizov, T. Dietl, S. Kolesnik, and M. Sawicki, Phase states and magnetic structure of superconducting lead inclusions in a narrow-gap PbTe semiconducting host, Semiconductors **32**, 700 (1998).

[16] K. Murase, S. Ishida, S. Takaoka, T. Okumura, H. Fujiyasu, A. Ishida, and M. Aoki, Superconducting behavior in PbTe-SnTe superlattices, Surf. Sci. **170**, 486 (1986).

[17] N. Ya. Fogel, E. I. Buchstab, Yu. V. Bomze, O. I. Yuzephovich, M. Yu. Mikhailov, A. Yu. Sipatov, E. A. Pashitskii, R. I. Shekhter, and M. Jonson, Direct evidence for interfacial superconductivity in two-layer semiconducting heterostructures, Phys. Rev. B **73**, 161306(R) (2006).

[18] S. Buchner, T. S. Sun, W. A. Beck, N. E. Byer, and J. M. Chen, Schottky barrier formation on (Pb,Sn)Te, J. Vac. Sci. Technol. **16**, 1171 (1979).

[19] W. Brzezicki, M. Wysokiński, and T. Hyart, Topological properties of multilayers and surface steps in the SnTe material class, arXiv:1812.02168.

[20] P. Sessi, D. Di Sante, A. Szczerbakow, F. Glott, S. Wilfert, H. Schmidt, T. Bathon, P. Dziawa, M. Greiter, T. Neupert, G. Sangiovanni, T. Story, R. Thomale, and M. Bode, Robust spin-polarized midgap states at step edges of topological crystalline insulators, Science **354**, 1269 (2016).

[21] D. Iaia, C.-Y. Wang, Y. Maximenko, D. Walkup, R. Sankar, Fangcheng Chou, Y.-M. Lu, and V. Madhavan, Topological nature of step edge states on the surface of the topological crystalline insulator $Pb_{0.7}Sn_{0.3}Se$, Phys. Rev. B **99**, 155116 (2019).

[22] C. M. Polley, R. Buczko, A. Forsman, P. Dziawa, A. Szczerbakow, R. Rechciński, B. J. Kowalski, T. Story, M. Trzyna, M. Bianchi, A. G. Čabo, P. Hofmann, O. Tjernberg, and T. Balasubramanian, Fragility of the Dirac cone splitting in topological crystalline insulator heterostructures, ACS Nano **12**, 617 (2018).

[23] R. Rechciński and R. Buczko, Topological states on uneven (Pb,Sn)Se (001) surfaces, Phys. Rev. B **98**, 245302 (2018).

[24] A. Szczerbakow and K. Durose, Self-selecting vapour growth of bulk crystals—Principles and applicability, Prog. Cryst. Growth Charact. Mater. **51**, 81 (2005).

[25] T. Story, R. R. Gałązka, R. B. Frankel, and P. A. Wolff, Carrier-Concentration-Induced Ferromagnetism in PbSnMnTe, Phys. Rev. Lett. **56**, 777 (1986).

[26] See Supplemental Material at http://link.aps.org/supplemental/10.1103/PhysRevB.100.041408 for additional information on the results of the structural and magnetic characterization, the search for bulk and precipitation superconductivity, point-contact spectroscopy in various settings and for different magnetic field orientations, and the effects of electric current pulses, which includes Refs. [55,56].

[27] C. M. Polley, V. Jovic, T.-Y. Su, M. Saghir, D. Newby, B. J. Kowalski, R. Jakiela, A. Barcz, M. Guziewicz, T. Balasubramanian, G. Balakrishnan, J. Laverock, and K. E. Smith, Observation of surface states on heavily indium-doped SnTe(111), a superconducting topological crystalline insulator, Phys. Rev. B **93**, 075132 (2016).

[28] K. Dybko, M. Szot, A. Szczerbakow, M. U. Gutowska, T. Zajarniuk, J. Z. Domagala, A. Szewczyk, T. Story, and W. Zawadzki, Experimental evidence for topological surface states wrapping around a bulk SnTe crystal, Phys. Rev. B **96**, 205129 (2017).

[29] N. Berchenko, R. Vitchev, M. Trzyna, R. Wojnarowska-Nowak, A. Szczerbakow, A. Badyla, J. Cebulski, and T. Story, Surface oxidation of SnTe topological crystalline insulator, Appl. Surf. Sci. **452**, 134 (2018).

[30] K. Chang, T. P. Kaloni, H. Lin, A. Bedoya-Pinto, A. K. Pandeya, I. Kostanovskiy, K. Zhao, Y. Zhong, X. Hu, Q.-K. Xue, X. Chen, S.-H. Ji, S. Barraza-Lopez, and S. S. P. Parkin, Enhanced spontaneous polarization in ultrathin SnTe films with layered antipolar structure, Adv. Mater. **31**, 1804428 (2019)

[31] H. J. M. Swagten, W. J. M. de Jonge, R. R. Gałązka, P. Warmenbol, and J. T. Devreese, Hole density and composition dependence of ferromagnetic ordering in Pb-Sn-Mn-Te, Phys. Rev. B **37**, 9907 (1988).

[32] T. Dietl, H. Ohno, F. Matsukura, J. Cibert, and D. Ferrand, Zener model description of ferromagnetism in zinc-blende magnetic semiconductors, Science **287**, 1019 (2000).

[33] T. Dietl and H. Ohno, Dilute ferromagnetic semiconductors: Physics and spintronic structures, Rev. Mod. Phys. **86**, 187 (2014).

[34] D. Daghero and R. S. Gonnelli, Probing multiband superconductivity by point-contact spectroscopy, Supercond. Sci. Technol. **23**, 043001 (2010).

[35] S. Sasaki, M. Kriener, K. Segawa, K. Yada, Y. Tanaka, M. Sato, and Y. Ando, Topological Superconductivity in $Cu_xBi_2Se_3$, Phys. Rev. Lett. **107**, 217001 (2011).

[36] S. Sasaki, Z. Ren, A. A. Taskin, K. Segawa, L. Fu, and Y. Ando, Odd-Parity Pairing and Topological Superconductivity in a Strongly Spin-Orbit Coupled Semiconductor, Phys. Rev. Lett. **109**, 217004 (2012).

[37] G. Sheet, S. Mukhopadhyay, and P. Raychaudhuri, Role of critical current on the point-contact Andreev reflection spectra between a normal metal and a superconductor, Phys. Rev. B **69**, 134507 (2004).

[38] J. Appelbaum, "*s-d*" Exchange Model of Zero-Bias Tunneling Anomalies, Phys. Rev. Lett. **17**, 91 (1966).

[39] P. W. Anderson, Localized Magnetic States and Fermi-Surface Anomalies in Tunneling, Phys. Rev. Lett. **17**, 95 (1966).

[40] Y. Meir, N. S. Wingreen, and P. A. Lee, Low-Temperature Transport Through a Quantum Dot: The Anderson Model Out of Equilibrium, Phys. Rev. Lett. **70**, 2601 (1993).

[41] M. Pustilnik and L. I. Glazman, Kondo Effect in Real Quantum Dots, Phys. Rev. Lett. **87**, 216601 (2001).

[42] A. L. Efros and B. I. Shklovskii, Coulomb gap and low temperature conductivity of disordered systems, J. Phys. C **8**, L49 (1975).

[43] B. L. Al'tshuler and A. G. Aronov, Contribution to the theory of disordered metals in strongly doped semiconductors, Zh. Eksp. Teor. Fiz. **77**, 2028 (1979) [Sov. Phys. JETP **50**, 968 (1979)].

[44] S. Kundu and V. Tripathi, Role of Hund's splitting in electronic phase competition in $Pb_{1-x}Sn_xTe$, Phys. Rev. B **96**, 205111 (2017).

[45] E. Tang and L. Fu, Strain-induced partially flat band, helical snake states and interface superconductivity in topological crystalline insulators, Nat. Phys. **10**, 964 (2014).

[46] T. Dietl, K. Sato, T. Fukushima, A. Bonanni, M. Jamet, A. Barski, S. Kuroda, M. Tanaka, P. N. Hai, and H. Katayama-Yoshida, Spinodal nanodecomposition in semiconductors doped with transition metals, Rev. Mod. Phys. **87**, 1311 (2015).

[47] W.-H. Li, C. C. Yang, F. C. Tsao, and K. C. Lee, Quantum size effects on the superconducting parameters of zero-dimensional Pb nanoparticles, Phys. Rev. B **68**, 184507 (2003).

[48] V. Yeh, S. Y. Wu, and W.-H. Li, Measurements of superconducting transition temperature T_c of Sn nanoparticles, Colloids Surf., A **313-314**, 246 (2008).

[49] K. Gas and M. Sawicki, In situ compensation method for high-precision and high-sensitivity integral magnetometry, Meas. Sci. Technol. **30**, 085003 (2019).

[50] R. T. Tung, The physics and chemistry of the Schottky barrier height, Appl. Phys. Rev. **1**, 011304 (2014).

[51] M. Górska and J. R. Anderson, Magnetic susceptibility and exchange in IV-VI compound diluted magnetic semiconductors, Phys. Rev. B **38**, 9120 (1988).

[52] K. Yu. Arutyunov, D. S. Golubev, and A. D. Zaikin, Superconductivity in one dimension, Phys. Rep. **464**, 1 (2008).

[53] J.-P. Pouget, The Peierls instability and charge density wave in one-dimensional electronic conductors, C. R. Phys. **17**, 332 (2016).

[54] A. J. Heeger, S. Kivelson, J. R. Schrieffer, and W.-P. Su, Solitons in conducting polymers, Rev. Mod. Phys. **60**, 781 (1988).

[55] M. Novak, S. Sasaki, M. Kriener, K. Segawa, and Y. Ando, Unusual nature of fully gapped superconductivity in In-doped SnTe, Phys. Rev. B **88**, 140502(R) (2013).

[56] T. Dietl, C. Śliwa, G. Bauer, and H. Pascher, Mechanisms of exchange interactions between carriers and Mn or Eu spins in lead chalcogenides, Phys. Rev. B **49**, 2230 (1994).